Results in Physics 12 (2019) 1826–1833

Contents lists available at ScienceDirect

Results in Physics

journal homepage: www.elsevier.com/locate/rinp

# Characterization of stress softening and self-healing in a double network hydrogel

İsmail Doğan Külcü

*Faculty of Engineering, Turkish-German University, Sahinkaya Cad. 86, 34820 Beykoz/Istanbul, Turkey*

ARTICLE INFO

*Keywords:*
Constitutive modeling
Stress softening
Self healing
Rubber-like materials
Tough hydrogels

ABSTRACT

In this paper, a micro-mechanically based constitutive model is presented to describe stress softening and self-healing in alginate-polyacrylamide (PAAm) double network (DN) hydrogels. The stress softening phenomenon in alginate-PAAm DN hydrogels under cyclical deformation is assumed to be the result of the rupture of chain linkages. Therefore, the network evolution method [Dargazany and Itskov, *International Journal of Solids and Structures*, 2009, **46**, 2967] is used to characterize stress softening. The polymer matrix is initially decomposed into reversible and irreversible polymer networks. To model stress softening, the entropic energy of a polymer chain and the chain distribution are taken into account for each network. Unlike conventional DN hydrogels, after deformation alginate-PAAm hydrogels show self-healing. The rate of self-healing is associated with both intermolecular forces and the duration of storage of the samples in a thermal chamber. Broken chain linkages are assumed to rebond due to intermolecular forces and heating. Chemical reaction kinetics and heat transfer equations are utilized to calculate the quantity of the reversible cross-linking rebonding. This model contains few material parameters and demonstrates good agreement with experimental data in stress softening and self-healing.

## 1. Introduction

Double network (DN) hydrogels are a class of tough hydrogels that consist of highly cross-linked polyelectrolyte and loosely cross-linked neutral polymer networks [1–6]. In addition to the general features of conventional hydrogels such as high water content and bio-compatibility, DN hydrogels are known for their extraordinary mechanical features [6,2,7,4,8]. Therefore, they become prominent candidates for the hydrogel load-bearing applications of cartilage, spinal cord, and bone [9–12].

Many hydrogel applications, in particular in the fields of medicine and biology, require toughness. One of the features that reveals the toughness of a material is the stress softening phenomenon. In addition to exhibiting tensile nominal stress up to 10 MPa, compressive nominal stress up to 60 MPa, fracture energy up to 1000 J/m$^2$ [2], DN hydrogels shows the stress softening under quasi-static loading [7]. It is crucial to describe stress softening to characterize the mechanical properties of DN hydrogels.

In the first constitutive modeling approaches of DN hydrogels [13,14], the highly cross-linked polyelectrolyte network is associated with damage evolution and stress softening. These models assume that the neutral network is a purely elastic material, and that crack propagation appears in the polyelectrolyte network resulting in a decrease in the stiffness of samples. Later, Wang and Hong [15] constituted a phenomenological model based on the Ogden-Roxburgh pseudo-elasticity model to describe the high fracture energy, the Mullins effect, and yielding of a DN hydrogel. Zhao [16] furthermore introduced a micro-mechanical model for a polymer matrix consisting of interpenetrating polymer networks. This model uses the Arruda-Boyce eight chain model [17] and the network alteration concept [18,19]. The polymer matrix is decomposed into short and long polymer chains, and the polymer network evolution under deformation takes place with respect to chain length. Recently, the relationship between viscoelastic behavior and DN hydrogel fracture to stress softening has also been studied [20,21].

The ability to repair without any external intervention is an outstanding feature of natural materials, such as natural rubber and soft tissues. This behavior is called *self-healing*. Recent advances in material science have demonstrated that man-made materials can mimic the self-healing. Self-healing mechanisms differ due to the structure of materials. Using a healing agent or altering the chemical structure to include reversible bond are two possible ways to produce such materials [22,23]. Although our understanding of self-healing behavior is enhanced, the physical and thermodynamic sources of these systems still give rise to many questions.

DN hydrogels, which are synthesized via covalent cross-linking, do not recover itself, unlike soft tissues and elastomers [24]. This

*E-mail address:* kulcu@tau.edu.tr.

https://doi.org/10.1016/j.rinp.2019.01.078
Received 13 December 2018; Received in revised form 17 January 2019; Accepted 28 January 2019
Available online 31 January 2019

drawback hampers the applicability of conventional DN hydrogels to load-bearing applications. To overcome the problem of irreversible damage in DN hydrogels after deformation, Sun et al. [25] developed an alginate-polyacrylamide (PAAm) DN hydrogel. Alginate, which is made up of ionic cross-links between divalent cations such as $Ca^{+2}$, is the polyelectrolyte network of the DN hydrogel. Ionic bonds are easier to reactivate than their covalent counterparts due to a lower activation energy required for the chemical reaction. When alginate-PAAm hydrogels are stored in a chamber and subjected to a heating process after a deformation cycle they exhibit self-healing behavior. This healing process is enhanced by increasing the temperature and duration of resting.

Alginate-PAAm DN hydrogels provide crucial insights into how to enhance the mechanical properties of DN hydrogels. As they potentially have the ability to heal themselves autonomously, they can be used in applications that require self-healing behavior in the fields of biology, medicine, and engineering [26–29]. It is therefore important to describe the behavior of this material during its healing process. Hui and Long [30] have proposed a model for an ionically cross-linked triblock copolymer hydrogel, where ionic cross-links are formed between polyelectrolyte mid-blocks due to ionic interactions. Their model involves a rate-independent recovery and is based upon the findings of Wang and Hong [15]. Later, Long et al. [31] presented a strain rate dependent phenomenological model for dual cross-linked self-healing polyvinyl alcohol (PVA) hydrogels, which are comprised of dual cross-links and are tough hydrogel. Recently, Guo et al. [32] have extended this work by representing a rate-dependent theory to describe the multi-axial behavior of gels consisting of different types. This recent work is novel in that it uses fewer material parameters based on the assumption of bond kinetics reaching a steady state of breaking and rebonding, and it demonstrates strain stiffening up to 400% strain.

In our present paper, a constitutive model is presented for stress softening and self-healing phenomena in alginate-PAAm DN hydrogels. To the best of our knowledge, the convergence in literature between modeling and experimental studies of the stress softening phenomenon of DN hydrogels under consecutive cyclical loading is poor. This work aims to provide a better understanding of these phenomena. Our modeling approach consists of two parts. First, to provide an insight into the damage mechanism of the material under deformation, the stress softening phenomenon is characterized. Then, based on the characterization of the internal damage shown in the first part, the self-healing behavior and recovery mechanism are studied.

## 2. Constitutive modeling

### 2.1. Modeling of stress softening

Stress softening, which is the deviation between the loading and unloading curves in the stress–strain diagram, is observed in different classes of tough hydrogels, like nanocomposite gels and DN hydrogels [33,34]. Starting with the works of Mullins and his collaborators in the 1950's [35–38], much research has been conducted, predominantly in the filled rubber-like materials, to characterize [39–53]. However, the reason for stress softening in elastomeric materials is still indistinct due to the very complicated structure of these polymers.

The network evolution method (NEM) [51] is a continuum approach that describes the polymer network evolution of elastomers under large deformation. In the NEM, damage in the polymer network results from the debonding of polymer chains from the filler surface [45,54]. The NEM is based on the network decomposition concept of Govindjee and Simo [46], where the polymer matrix is split into cross-link-to-cross-link (CC) and particle-to-particle (PP) polymer networks. The CC network is hyperelastic. Deformation evolution occurs in the PP network at the point where a chain is fully stretched. The network alteration theory by Marckmann et al. [18] takes network reorientation into account.

The damage in a DN hydrogel is considered as the rupture of cross-links [24,13]. Consequently, energy dissipation under cyclical deformation is assumed to result from only the energy used to debond chains from each other. Based on these assumptions, the NEM is used to describe the micro-mechanical basis of stress softening in DN hydrogels [55].

#### 2.1.1. Network decomposition

A DN hydrogel that exhibits stress softening and self-healing, consists of two types of cross-linking: reversible ionic and irreversible covalent. Thus, the strain energy of hydrogel matrices $\bullet_M$ can be investigated by the decomposition of the hydrogel matrix into reversible $\bullet_r$ and irreversible $\bullet_{ir}$ polymer networks as follows:

$$\Psi_M = \Psi_r + \Psi_{ir}, \tag{1}$$

where $\Psi$ is the strain energy function. Additionally, two different types of covalent bonds exist in alginate-PAAm DN hydrogels. One results in cross-linking within the PAAm network, while the other results in cross-linking between alginate and PAAm networks. Thus, Eq. (1) can be rewritten as

$$\Psi_M = \Psi_r + \Psi_{ir,n} + \Psi_{ir,int}, \tag{2}$$

where subscripts $\bullet_{ir,n}$ and $\bullet_{ir,int}$ represent the PAAm network and the interaction between the alginate and PAAm networks, respectively.

Considering the number of active chains in a network $N$, the energy of the DN hydrogel matrix is rewritten as

$$\Psi_M = N_r\psi_r + N_{ir,n}\psi_{ir,n} + N_{ir,int}\psi_{ir,int}, \tag{3}$$

where $\psi$ is the entropic energy of a single chain. $\psi$ is written based on non-Gaussian statistics as

$$\psi = kTn\left(\frac{\bar{r}}{n}\beta + \ln\frac{\beta}{\sinh\beta}\right), \tag{4}$$

where $\beta = \mathscr{L}^{-1}\left(\frac{\bar{r}}{n}\right)$ is the inverse Langevin function, $k$ is the Boltzmann constant, $T$ is the absolute temperature, $\bar{r} = \frac{r}{l}$ is the normalized mean end-to-end distance of a chain with respect to the length of a segment $l$ and $n$ is the segment number of a chain. To approximate the inverse Langevin function, $\mathscr{L}^{-1}(y) = \frac{3y}{1-y^3}$ [56] is used.

Furthermore, by integrating over the set of available chains $D^A$, the strain energy of chains in a particular direction $\boldsymbol{d}$ is formulated as

$$\overset{\boldsymbol{d}}{\Psi}_M = \int_{D_r^A} N_r \overset{\boldsymbol{d}}{\psi}_r \mathrm{d}n + \int_{D_{ir,n}^A} N_{ir,n} \overset{\boldsymbol{d}}{\psi}_{ir,n} \mathrm{d}n + \int_{D_{ir,int}^A} N_{ir,int} \overset{\boldsymbol{d}}{\psi}_{ir,int} \mathrm{d}n. \tag{5}$$

#### 2.1.2. Probability density of a chain existence

With respect to the length of the polymer chains, deformation is assumed to occur from the shortest chains to longest ones [53,52] (see Fig. 1). To define the chain existence and describe the deformation evolution in a polymer network, a probability density function is considered over set of available chains $D^A$, which is written as

$$D^A = \{n | n_{min}\lambda \leqslant n \leqslant n_{max}\}, \tag{6}$$

where $\lambda$, $n_{min}$ and $n_{max}$ are the micro-stretch and the minimum and maximum segment numbers, respectively. The variable $n_{max}$ is taken as a material parameter. The shortest chain length is equal to the contour length of a chain, and express the deformation in a network (see Fig. 1). The variable $n_{min}$ over $D^A$ is represented as

$$n_{min} = \nu\bar{r}, \tag{7}$$

where $\nu$ is the sliding ratio (see [51]).

The Gaussian probability density function (PDF) is adequate, if the distribution of the chain length in a polymer network is assumed to be random. Assuming a chain with $i$ number of segments that is cross-linked at the $i$th segment while previous segments are never cross-linked, the PDF of the chain length (cf. [46,52]) is represented as

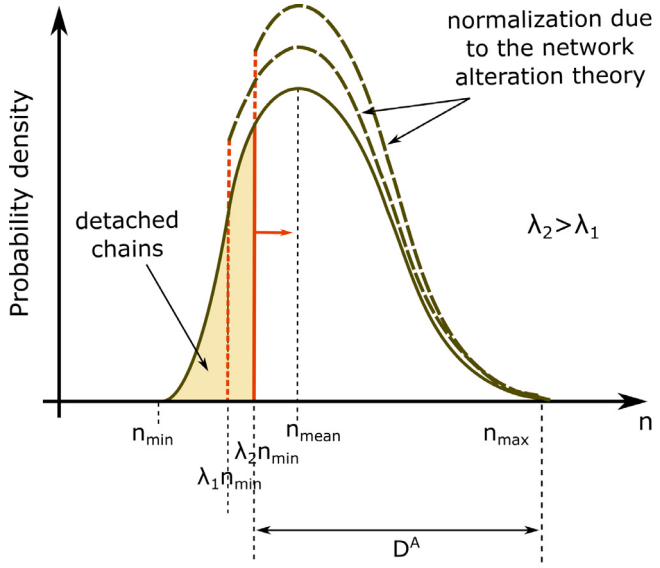


**Fig. 1.** Schematic view of the probability density.

$$P\left(n, \bar{r}, \kappa\right) = \kappa\sqrt{\frac{6}{\pi n}}\, e^{B}, \tag{8}$$

where

$$B = -A - \kappa\sqrt{\frac{24}{\pi}}\left[\sqrt{An\pi}\left[\operatorname{erf}(\sqrt{A}) - \operatorname{erf}(\sqrt{An})\right] + \sqrt{n}\, e^{-A} - e^{-An}\right], \tag{9}$$

$$A = \frac{3\bar{r}^2}{2n}. \tag{10}$$

where $\kappa$ is the density of the cross-linking site of a polymer network and is proportional to the cross-linking density of the overall polymer network [45,52]. As there exists no particle in the polymer network, the adsorption site separation distribution is not used, unlike Govindjee and Simo [46].

### 2.1.3. Network reorganization

A polymer chain can be attached at many segments along its length due to the highly complicated structure of polymer networks. Therefore, the rupture of a cross-link does not necessarily cause the complete loss of the role of the chain in the entropic energy [52]. The shortest attachment on a chain is considered to be active, whereas longer ones are considered as de-active and they do not bear loads [51]. The rupture of a short linkage activates longer linkages (see Fig. 2). Breakage of the longest linkage cause dangling chains, which do not carry load. Thus, introducing both the total number of active chains $N_a$ in a network and the normalization function $f\left(\overset{d}{\lambda}_m\right)$, the number of fully stretched chains at a point in the deformed network is written (see [52]) as

$$\begin{aligned} N(n, \bar{r}, \kappa) &= N_a(\bar{r}) f\left(\overset{d}{\lambda}_m\right) P\left(n, \bar{r}, \kappa\right) \\ &= \widetilde{N}\left(\overset{d}{\lambda}_m \bar{r}\right) P\left(n, \bar{r}, \kappa\right). \end{aligned} \tag{11}$$

The network alteration theory (NAT) of Marckmann et al. [18] has been presented to consider the re-organization of polymer matrix after the deformation. Network alteration theory represents the constant active segment number in a polymer network at any stage of the deformation as

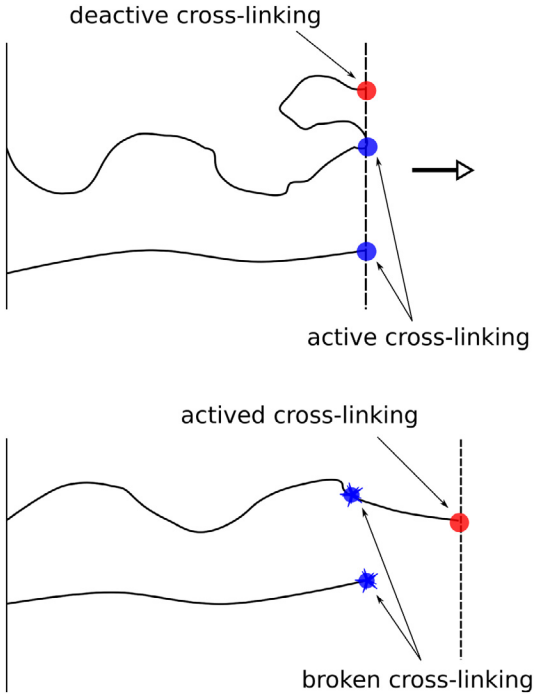


**Fig. 2.** Organization of polymer chains under deformation.

$$\int_{D^A(\overset{d}{\lambda_i})} \widetilde{N}\left(\overset{d}{\lambda_i}\right) nP\left(n, \bar{r}, \kappa\right) \mathrm{d}n = \int_{D^A(\overset{d}{\lambda_j})} \widetilde{N}\left(\overset{d}{\lambda_j}\right) nP\left(n, \bar{r}, \kappa\right) \mathrm{d}n. \tag{12}$$

where $(i \neq j)$.

Let us assume a virgin network $(i = 1)$ as

$$\widetilde{N}\left(\overset{d}{\lambda_j}\right) = \frac{\widetilde{N}\left(\overset{d}{\lambda_1}\right) \int_{D^A(\overset{d}{\lambda_1})} nP\left(n, \bar{r}, \kappa\right) \mathrm{d}n}{\int_{D^A(\overset{d}{\lambda_j})} nP\left(n, \bar{r}, \kappa\right) \mathrm{d}n}. \tag{13}$$

The nominator of Eq. 13 is shown (see [52,57]) as

$$N_0 = \widetilde{N}\left(\overset{d}{\lambda_1}\right) \int_{D^A(\overset{d}{\lambda_1})} nP\left(n, \bar{r}, \kappa\right) \mathrm{d}n, \tag{14}$$

where $N_0$ is the active chain number in an undeformed network. The value of $N_0$ due to the polymerization process of a network is calculated as

$$N_0 = a\frac{N_A M}{n_{mean}}, \tag{15}$$

where $N_A$ is Avagadro's constant, $M$ is the molar ratio of the network, $n_{mean}$ is the mean segment number that is obtained from the probability distribution (see Fig. 1), and $a$ is the active chain ratio in the network.

The present model is limited to the rubber elasticity, and viscoelastic effects are neglected. Thus, the number of broken chain linkages in a network is calculated assuming that the dissipated energy results only from the rupture of cross-links. Therefore, $a$ is calculated by calculating energy dissipation under cyclic deformation (see [24,7,8]). Finally, the number of active chains at any point of the deformation is written as

$$\widetilde{N}\left(\overset{d}{\lambda_j}\right) = N_0 \Phi\left(\overset{d}{\lambda_j}\right), \tag{16}$$

where

$$\Phi\left(\overset{d}{\lambda_j}\right) = \left(\int_{D^A(\overset{d}{\lambda_j})} nP\left(n, \bar{r}, \kappa\right) \mathrm{d}n\right)^{-1}. \tag{17}$$

*2.1.4. Energy of a deformed network*

The energy of a loaded chain in the direction $\boldsymbol{d}$ is written as

$$\overset{\boldsymbol{d}}{\psi} = \psi(n, \overset{\boldsymbol{d}}{\lambda}\bar{r}). \tag{18}$$

To calculate the free energy of the deformed network ($\Psi$), the relative end-to-end direction $\boldsymbol{d}$ and the number of active chains over $D^A$ are taken into account using

$$\begin{aligned}\overset{\boldsymbol{d}}{\Psi} &= \int_{D^A(\overset{\boldsymbol{d}}{\lambda_m})} N\left(n, \bar{r}, \kappa\right)\psi(n, \overset{\boldsymbol{d}}{\lambda}\bar{r})\mathrm{d}n \\ &= \int_{D^A(\overset{\boldsymbol{d}}{\lambda_m})} \widetilde{N}(\overset{\boldsymbol{d}}{\lambda_m})P\left(n, \bar{r}, \kappa\right)\psi(n, \overset{\boldsymbol{d}}{\lambda}\bar{r})\mathrm{d}n,\end{aligned} \tag{19}$$

where $\overset{\boldsymbol{d}}{\lambda}_m$ is micro-stretch in the direction $\boldsymbol{d}$.

Substituting Eqs. (15) and (16) into 19, the energy of a network in the direction $\boldsymbol{d}$ is written as

$$\overset{\boldsymbol{d}}{\Psi} = a\frac{N_A M}{n_{mean}}\Phi(\overset{\boldsymbol{d}}{\lambda_m})\int_{D^A(\overset{\boldsymbol{d}}{\lambda_m})} P\left(n, \bar{r}, \kappa\right)\psi(n, \overset{\boldsymbol{d}}{\lambda}\bar{r})\mathrm{d}n. \tag{20}$$

*2.1.5. Generalization of the one-dimensional model to three-dimensions*

The undeformed DN hydrogel network is assumed to be homogenous and isotropic in all directions. The free energy of a DN hydrogel matrix is considered to be the sum of the strain energies of chains in all directions. Also, during reorganization of chains due to the network alteration theory, directions are taken to remain unchanged. Thus, the concept of the numerical integration scheme over the unit sphere is used to generalize the model from one dimension to three dimensions. The numerical scheme of Bažant and Oh [58] is taken into account. Thus, the equation for the energy of the networks in three dimensions for reversible and irreversible polymer networks is written as

$$\Psi = \frac{1}{4\pi}\int_S \overset{\boldsymbol{d}}{\Psi}_{r,ir}\mathrm{d}\overset{\boldsymbol{d}}{u} = \sum_{i=1}^{21} \omega_i \overset{\boldsymbol{d}_i}{\Psi}_{r,ir}. \tag{21}$$

where $\omega_i$ represents the weight factor.

*2.1.6. Constitutive equation*

The first Piola-Kirchhoff stress tensor $\mathbf{P}$ of alginate-PAAm hydrogel is written using Eq. 2 as

$$\mathbf{P} = \frac{\partial\Psi_M}{\partial\mathbf{F}} = \frac{\partial\Psi_r}{\partial\mathbf{F}} + \frac{\partial\Psi_{ir,n}}{\partial\mathbf{F}} + \frac{\partial\Psi_{ir,int}}{\partial\mathbf{F}} - p\mathbf{F}^{-T}, \tag{22}$$

where $\mathbf{F}$ is the deformation gradient.

The affine deformation for polymer networks is considered. Thus, the strain amplification observed in filled elastomers is neglected, and assume that the micro-stretch and macro-stretch are equal. By using Eq. 20 and integrating over the unit sphere for the transition of the model from one-dimension to three dimensions, one can formulate the evolution equation for alginate-PAAm hydrogels as

$$\begin{aligned}\mathbf{P} &= \sum_{i=1}^{21}\omega_i\left[\frac{\frac{\partial\Psi_r}{\partial\lambda}}{\boldsymbol{d}_i} + \frac{\frac{\partial\Psi_{ir,n}}{\partial\lambda}}{\boldsymbol{d}_i} + \frac{\frac{\partial\Psi_{ir,int}}{\partial\lambda}}{\boldsymbol{d}_i}\right]\frac{1}{\lambda}\mathbf{F}\left(\boldsymbol{d}_i \otimes \boldsymbol{d}_i\right) - p\mathbf{F}^{-T} \\ &= \sum_{i=1}^{21}\omega_i\left[N_r(\overset{\boldsymbol{d}}{\lambda_m})\int_{D_A^r(\overset{\boldsymbol{d}}{\lambda_m})} P\left(n, \bar{r}_r, \kappa_r\right)\frac{\partial\psi(n,\bar{r}_r\lambda)}{\partial\lambda}\mathrm{d}n\right. \\ &+ N_{ir,n}(\overset{\boldsymbol{d}}{\lambda_m})\int_{D_A^{ir,n}(\overset{\boldsymbol{d}}{\lambda_m})} P\left(n, \bar{r}_{ir,n}, \kappa_{ir,n}\right)\frac{\partial\psi(n,\bar{r}_{ir,n}\lambda)}{\partial\lambda}\mathrm{d}n \\ &\left.+ N_{ir,int}(\overset{\boldsymbol{d}}{\lambda_m})\int_{D_A^{ir,int}(\overset{\boldsymbol{d}}{\lambda_m})} P\left(n, \bar{r}_{ir,int}, \kappa_{ir,int}\right)\frac{\partial\psi(n,\bar{r}_{ir,int}\lambda)}{\partial\lambda}\mathrm{d}n\right] \\ &\frac{1}{\lambda}\mathbf{F}\left(\boldsymbol{d}_i \otimes \boldsymbol{d}_i\right) - p\mathbf{F}^{-T}.\end{aligned} \tag{23}$$

*2.2. Modeling of self-healing*

Self-healing is the improvement of the mechanical behavior of materials after deformation cycles. To enhance the mechanical behavior of deformed alginate-PAAm DN hydrogels, Sun et al. [25] sealed samples in a polyethylene bag and immersed them in a mineral oil to prevent the evaporation of water. These samples were then stored in a thermal chamber for varying time durations. This heating process in the thermal chamber prompts a chemical reaction, where the reattachment of polymer chains can occur. In addition to external energy sources such as heating, a chemical reaction may appear from internal sources such as intermolecular forces. The present modeling of the self-healing of DN hydrogels accounts for both these sources.

The amount of energy transferred to samples, and thus the enhancement of their self-healing behavior of samples is proportional to the durations the samples were stored in the chamber. Therefore, the energy generated from energy sources is associated with the number of rebonded cross-links. The chemical process to rebond a cross-link requires an activation. To relate the activation energy to the energy generated from energy sources, the total quantity of rebonded cross-links $\mathscr{K}$ in a deformed network is presented as

$$\mathscr{K} = \frac{U_{source}}{U_a}, \tag{24}$$

where $U_{source}$ and $U_a$ are the energy coming from energy sources and the activation energy of the chemical process, respectively. $\mathscr{K}$ is decomposed as

$$\mathscr{K} = \mathscr{K}_{ext} + \mathscr{K}_{int}, \tag{25}$$

where $\mathscr{K}_{ext}$ and $\mathscr{K}_{int}$ represent the total quantity of rebonded cross-links due to external and internal energy resources, respectively.

*2.2.1. Internal energy sources*

Even when there is no external source to prompt chemical reactions, they can still occur in the system due to inter-molecular forces. The chemical reaction rate (CRR), which is related to internal kinetics and the energy potential of the sample, is considered as the internal energy source. The total quantity of rebonded cross-links due to the internal energy source of the sample $\mathscr{K}_{int}$ is decomposed as

$$\mathscr{K}_{int} = \mathscr{K}_{int,1} + \mathscr{K}_{int,2}.$$

where $\mathscr{K}_{int,1}$ and $\mathscr{K}_{int,2}$ are re-bonded cross-linking parameters for the CRR and the energy potential of a sample, respectively.

The thermal energy of molecules induces the CRR, which is linked to the reaction kinetics of the reactant molecules. The CRR, is defined by the Arrhenius equation that is based on collision theory as

$$k(T) = \mathscr{A}\mathrm{e}^{-\frac{U_a}{RT}}, \tag{26}$$

where $k$, $R$, $T$ and $A$ are the rate constant, gas constant, absolute temperature, and pre-exponential factor, respectively. Eq. 26 demonstrates that the chemical reaction slows as the activation energy increases. Thus, the activation energy is calculated as

$$U_a = \frac{R\ln\frac{k_j}{k_i}}{\frac{1}{T_i} - \frac{1}{T_j}}, \tag{27}$$

where subscripts $\bullet_i$ and $\bullet_j$ denote the chemical reactions at different temperatures. Normalization of the work of the second loading by the work of the primary loading (see [25]) is associated with the CRR and is used to approximate the activation energy for a bond between the ionic divalent cation ($Ca^{+2}$) and the gluconate anion. $U_a$ is calculated to fall within 11 and 33.5 kJ.

The pre-exponential factor $\mathscr{A}$, also known as the frequency factor, is based on the frequency of collisions between reactant molecules and written as

$$\mathscr{A} = Zp, \tag{28}$$

where $Z$ and $p$ denote the collision factor and the steric factor, respectively. The frequency factor $\mathscr{A}$ can be defined using Coats-Redfern, MacCallum-Tanner or Horowitz-Metzger methods. In literature, value of $\mathscr{A}$ given for calcium oxilate ranges wide from $5.5{\cdot}10^5$ to $1.9{\cdot}10^{23}$ due to different heating rates [59].

Finally, one can define the reaction rate per unit mole using Eq. 26 as the number of reactions that appear to reactivate broken cross-links. If all reactions lead to cross-link re-bonding, the parameter for the total quantity of re-bonded cross-links per unit time $\mathscr{K}_{int,1}'$ due to $k$ is written as

$$\mathscr{K}_{int,1}'\left(T,\, t\right) = \frac{1}{N_A} k_i\left(T(t)\right). \tag{29}$$

Consequently, the parameter for the total quantity of re-bonded cross-links due to internal kinetic energy $\mathscr{K}_{int,1}$ is presented as

$$\mathscr{K}_{int,1} = \sum_{i=1}^{t_A} \mathscr{K}_{int,1}'. \tag{30}$$

The ability of a material to exhibit self-healing is dependent on the energy potential of the sample. This energy potential $U_{int,2}$ at $T_0$ is written as

$$U_{int,2}(T) = mcT_0, \tag{31}$$

where $m$ and $c$ are the mass and the specific heat capacity of the sample. The quantity of rebonded cross-links due to the internal energy stored $\mathscr{K}_{int,2}$ at temperature $T$ is written as

$$\mathscr{K}_{int,2}(T) = \frac{U_{int,2}(T)}{U_a}. \tag{32}$$

### 2.2.2. External energy sources

External energy sources, such as heat and light, generally act as catalysts to increase the rate of chemical reactions. In our modeling, the heating process is considered to be one of the reasons for the differing self-healing behaviors of alginate-PAAm hydrogel samples at different temperatures and different heating durations, and is addressed a heat transfer problem from an oven at $T_\infty$ °C to the sample at $T_0$ °C. The heating processes involved are assumed to be convection and radiation (see Fig. 3). Therefore, the total energy generated by the chamber per unit time $U_{st}$ from heat transfer as a sum of the energy of convection $U_{conv}$ and radiation $U_{rad}$ at time $t$ is presented as

$$\begin{aligned} U_{st} &= U_{conv} + U_{rad} \\ \rho V c \frac{dT}{dt} &= -\left(hA(T - T_\infty) + \epsilon\sigma_b(T^4 - T_\infty^4)\right), \end{aligned} \tag{33}$$

The total energy generated by the thermal chamber $U_{ht}$ is written as

$$U_{ht}\left(T,\, t\right) = \sum_{i=1}^{t_A} U_{st}\left(T(t_i)\right), \tag{34}$$

where $t_A$ is the healing duration. Let us assume that the alginate-PAAm hydrogel is a closed system, the temperature in the sample is uniform, and $U_{ht}(T,\, t)$ is used entirely to re-bond the broken cross-links. Thus, the parameter of the total quantity of re-bonded cross-links due to external energy sources can be written as

$$\mathscr{K}_{ext}(T) = \frac{U_{ht}(T,\, t)}{U_a}. \tag{35}$$

Finally, using Eq. 35, 29 and 32, the parameter of total quantity of re-bonded cross-links is expressed as

$$\begin{aligned} \mathscr{K}(T,\, t) &= \mathscr{K}_{ext}(T,\, t) + \mathscr{K}_{int}(T,\, t) \\ &= \mathscr{K}_{ext}(T,\, t) + \mathscr{K}_{int,1}(T,\, t) + \mathscr{K}_{int,2}(T) \\ &= \frac{1}{U_a}\left[\sum_{i=1}^{t_A} -\left(hA\left(T_i - T_\infty\right) + \epsilon\sigma_b\left(T_i^4 - T_\infty^4\right)\right) + mcT_0\right] \\ &\quad + \frac{1}{N_A}\sum_{i=1}^{t} k_i(T). \end{aligned} \tag{36}$$

The dependency of $\mathscr{K}$ on time and temperature is illustrated in Fig. 4. Increasing the healing time and/or the temperature increases the self-healing parameter. The variables in $t_A$ and $T$ are used as in the experimental data shown in [25].

### 2.3. Conformation of polymer chains after healing

In a load-free sample, the reattachment of de-bonded chains can be considered in two ways: reattachment from longer chain to the shorter chains (see Fig. 5-a), and random reattachment (see Fig. 5-b). The random reattachment is used in the modeling of self-healing as it is physically more feasible for an interpenetrating polymer network. In a random reattachment, the probability distribution remains unchanged. However, the number of active chains and the number of cross-links are changed due to the healing parameter. The number of broken chains $\check{N}$ during primary loading is written as

$$\check{N} = \widetilde{N}(\lambda_m)^{\boldsymbol{d}} \int_{(\lambda_m)}^{\boldsymbol{d}} P\left(n,\, \bar{r},\, \kappa\right) \mathrm{d}n. \tag{37}$$

Therefore, the number of reattached chains in the healing network is represented as

$$N_{r,heal} = \mathscr{K}\check{N}_r. \tag{38}$$

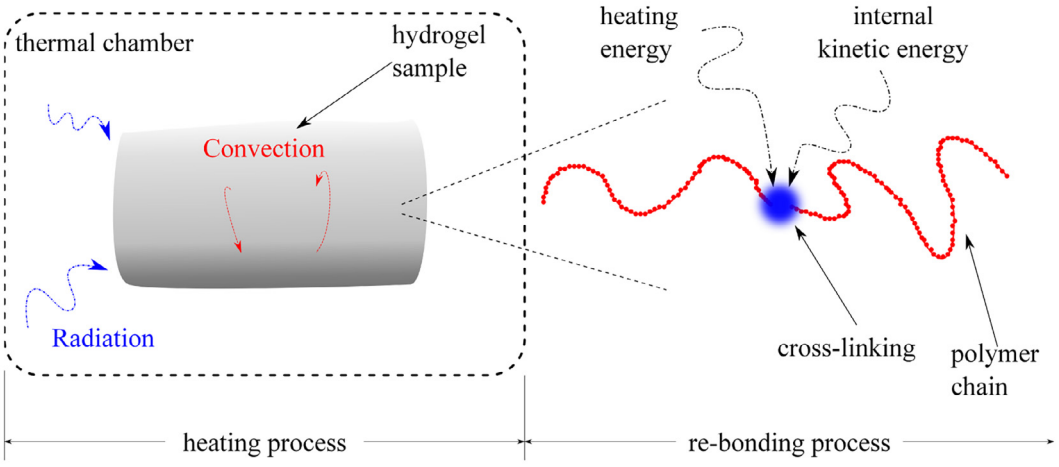


**Fig. 3.** Illustration of heating and re-bonding processes.

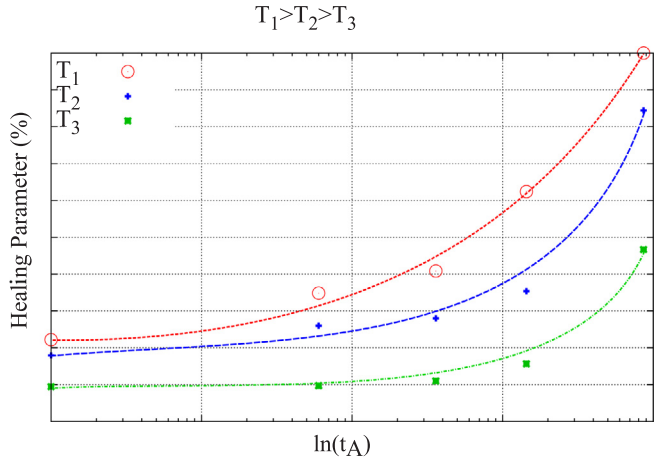


**Fig. 4.** Illustration of $\mathscr{K}$ at different temperatures for time different durations that is represented in the experimental data of Sun et al. [25].

Also, the density of the cross-link site $\kappa$ for the reversible network in the model is represented as

$$\kappa_{r,heal} = \mathscr{K}\kappa_r, \tag{39}$$

where $\kappa_{heal}$ is the material parameter $\kappa$ after healing.

### 2.4. Reloading

In addition to the self-healing network, the alginate-PAAm hydrogel matrix contains two irreversibly cross-linked damaged network during re-loading. Also, the reversibly cross-linked network may still contain damaged chains due to the healing parameter. Therefore, strain energy of the hydrogel matrix after healing $\hat{\Psi}$ is written as,

$$\hat{\Psi}_M = \underbrace{\mathscr{K}\Psi_r}_{\hat{\Psi}_r} + \left(1-\mathscr{K}\right)\breve{\Psi}_r + \breve{\Psi}_{ir,n} + \breve{\Psi}_{ir,int}, \tag{40}$$

where $\hat{\Psi}$ is the strain energy of healed network, $\breve{\Psi}_r$, $\breve{\Psi}_{ir,n}$ and $\breve{\Psi}_{ir,int}$ denote the strain energies of damaged networks during re-loading, respectively. Considering $\dot{\lambda}_m = 0$ during unloading, $\dot{\lambda}_m > 0$ during primary loading and reloading and the numerical scheme of integration over the unit sphere by Bažant and Oh [58] for the three-dimensional strain energy, one can rewrite $\hat{\Psi}_M$ as

$$\begin{aligned}\hat{\Psi}_M = \sum_{i=1}^{21} \omega_i \Bigg[ & \mathscr{K} N_r(\overset{d}{\lambda}_m) \int_{D_A^r(\overset{d}{\lambda}_m)} P\left(n, \bar{r}_r, \mathscr{K}\kappa_r\right)\psi\left(n, \lambda_m \bar{r}_r\right)\mathrm{d}n \\ & + \left(1-\mathscr{K}\right) N_r(\overset{d}{\lambda}_m) \int_{D_A^r(\overset{d}{\lambda}_m)} P\left(n, \bar{r}_r, \kappa_r\right)\psi\left(n, \lambda_m^{max} \bar{r}_r\right)\mathrm{d}n \\ & + N_{ir,n}(\overset{d}{\lambda}_m) \int_{D_A^{ir,n}(\overset{d}{\lambda}_m)} P\left(n, \bar{r}_{ir,n}, \kappa_{ir,n}\right)\psi\left(n, \lambda_m^{max} \bar{r}_{ir,n}\right)\mathrm{d}n \\ & + N_{ir,int}(\overset{d}{\lambda}_m) \int_{D_A^{ir,int}(\overset{d}{\lambda}_m)} P\left(n, \bar{r}_{ir,int}, \kappa_{ir,int}\right)\psi\left(n, \lambda_m^{max} \bar{r}_{ir,int}\right)\mathrm{d}n \Bigg], \end{aligned} \tag{41}$$

where $\lambda_m^{max}$ is the maximum stretch applied in the primary loading cycle. Thus, the evolution equation during self-healing is written as, The first Piola–Kirchhoff stress tensor with respect to the incompressibility condition is written as

$$\mathbf{P} = \frac{\partial \Psi_M}{\partial \mathbf{F}} = \mathscr{K}\frac{\partial \Psi_r}{\partial \mathbf{F}} + \left(1-\mathscr{K}\right)\frac{\partial \breve{\Psi}_r}{\partial \mathbf{F}} + \frac{\partial \breve{\Psi}_{ir,n}}{\partial \mathbf{F}} + \frac{\partial \breve{\Psi}_{ir,int}}{\partial \mathbf{F}} - p\mathbf{F}^{-T}. \tag{42}$$

## 3. Results and discussion

The present model is validated against the experimental self-healing alginate-PAAm hydrogel data [25]. The alginate-to-acrylamide ratio in this study was 1:6 ($M_r = 1$, $M_{ir,n} = 6$). As the cross-linking density of the polyelectrolyte network is larger than its neutral counterpart, the chain length of the polyelectrolyte network is assumed to be smaller. Thus, $\bar{r}_r < \bar{r}_{ir}$ and $\kappa_r > \kappa_{ir}$. Furthermore, in order to simplify the fitting procedure, the mean values of material parameters for alginate and PAAm ($\bar{r}_{ir,int} = (\bar{r}_r + \bar{r}_{ir,n})/2$ and $\kappa_{ir,int} = (\kappa_r + \kappa_{ir,n})/2$) were used for the material parameters for the network of interactions between alginate and PAAm.

Toughness is related to cross-link debonding at over 1000 J m$^{-2}$, which is similar to conventional DN hydrogels [2]. Therefore, assuming that all active chains are broken until the end of deformation, the active chain ratio $a$ can be up to 0.01 as shown by Webber et al. [24] in conventional DN hydrogels.

The material parameters used to validate the model under cyclical loading were obtained using the Levenberg-Marquardt algorithm.and are displayed in Table 1.

Two independent loading cycles were validated, and found that the present model exhibited a high level of agreement with experimental data (see Fig. 6-a). The behavior of individual networks in the model is presented in Fig. 6-b with the reversible network contributing to the stress significantly, and the energy dissipation in this network is

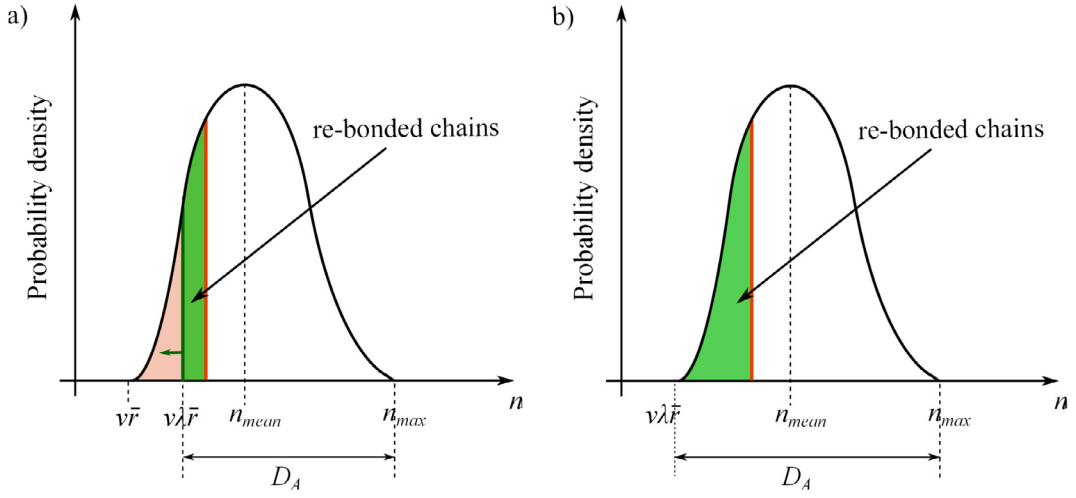


**Fig. 5.** Schematic view of the probability density of rebonded chains after the healing process. a) Reattachment from longer chains to shorter ones. b) Random reattachment.

**Table 1**
Material parameters for the stress softening of alginate-PAAm DN hydrogel.

| $\bar{r}_r$ | $\bar{r}_{ir,n}$ | $\kappa_r$ | $\kappa_{ir,n}$ | $n_{max}$ | $\nu$ | $a$ |
|---|---|---|---|---|---|---|
| 6.5 | 12 | 100.5 | 25 | 300 | 1.035 | 0.005 |

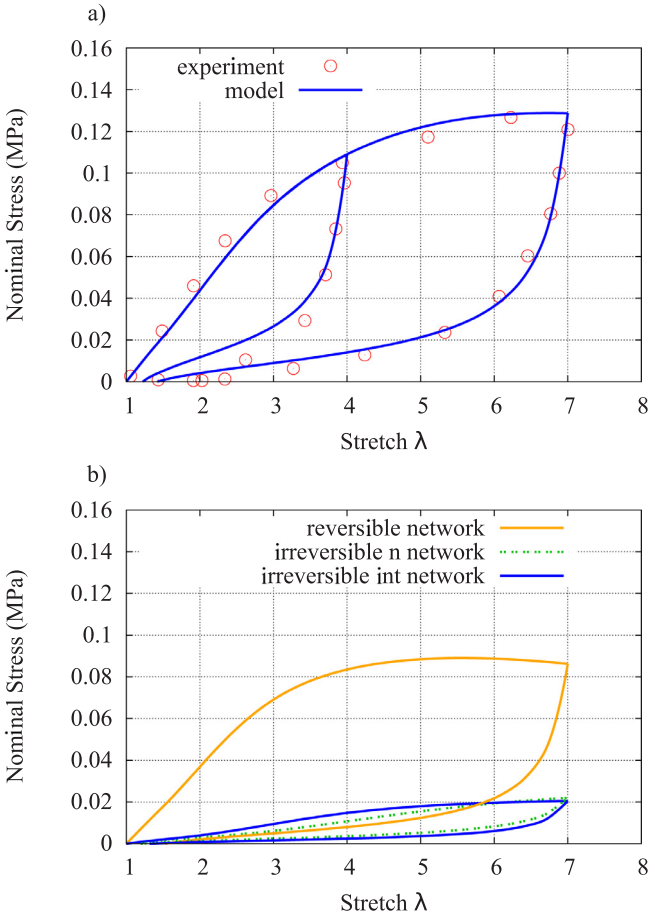


**Fig. 6.** a) Comparison of the stress softening model for two independent first loading cycles against experimental data of DN hydrogel showing self-healing behavior. b) Behavior of the individual networks in the model.

**Table 2**
Material parameters used the modeling of alginate-PAAm DN hydrogel self-healing.

| h | c | ϵ | A |
|---|---|---|---|
| 20,000 | 4.1813 | 0.83 | $4.3 \cdot 10^{20}$ |

significantly higher than in other parts. The influence of PAAm is relatively smaller due to its long and loosely cross-linked polymer structure.

To investigate self-healing behavior, the values shown in Table 2 were used for the material parameters. The values of $h$, $c$ and $\epsilon$ are associated with the properties of water. The mean value of $U_a$ (22 kJ) is used within the range represented in subSection 2.2.1. For the reaction of $Ca^{+2}$ with guluronic acid, $A$ is in the range mentioned in subSection 2.2.

Fig. 7 shows the comparison between the results of the self-healing model with those of experimental data observed at different time durations. Good agreement is observed between the model and experimental data.

It should be noted that as it is difficult to cut dumbbell shape

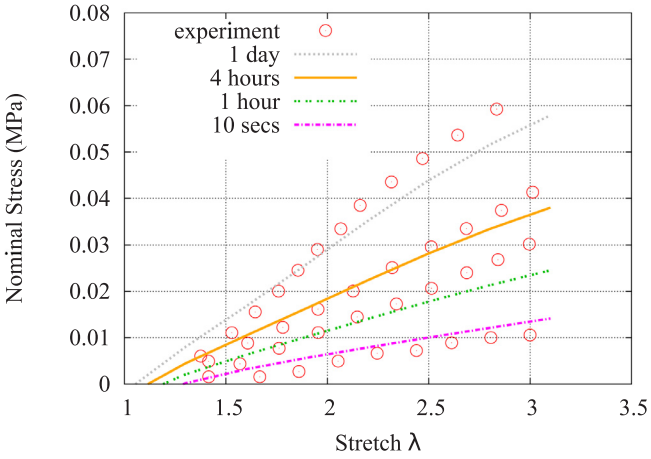


**Fig. 7.** Self-healing behavior at 80 °C at different time durations of samples in a thermal chamber between tests.

samples and clamp them due to the sticky structure of hydrogels. International tensile test standards for rubber-like materials were not followed in the experimental procedure of alginate-PAAm hydrogels in the studies of [60,25]. Therefore, more detailed experimental studies for these hydrogels are required. Also, the viscoelastic dissipation during deformation and healing and the energy loss while calculating the energy transfer from chamber to sample have been neglected. Taking the viscoelastic properties of materials into account and conducting the heat transfer experiments in detail may allow the application of our model at higher strain values.

## 4. Conclusion

Recent experimental studies reveal that DN hydrogels, unlike conventional hydrogels, exhibit stress softening that is similar to one observed in filled rubber-like materials and self-healing [25]. The motivating key for this work was the absence of constitutive models that could micro-mechanically characterize experimental data on the stress softening and the self-healing. Thus, in the present paper a purely micro-mechanical model is proposed to understand the internal damage and recovery mechanism inside an alginate-PAAm DN hydrogel. The model is presented in two stages: the stress softening and the self-healing. The modeling of the stress softening is carried out based on the network evolution method by Dargazany and Itskov [51]. The evolution equation is obtained based on the dissipated energy to break cross-linking of chains and the chain orientation during and after deformation to describe the stress softening. The self-healing is calculated based on internal kinetics and the heating energy that subjects to the alginate-PAAm hydrogel sample in the thermal chamber. The model contains few material parameters, which all have a physical interpretation. The good performance is achieved in the modeling of stress softening and self-healing.

## References

[1] Haque MA, Kurokawa T, Gong JP. Super tough double network hydrogels and their application as biomaterials. Polymer 2012;53:1805–22.
[2] Gong JP. Why are double network hydrogels so tough? Soft Matter 2010;6:2583–90.
[3] Nakajima T, Furukawa H, Tanaka Y, Kurokawa T, Osada Y, Gong JP. True chemical structure of double network hydrogels. Macromolecules 2009;42:2184–9.
[4] Na Y, Tanaka Y, Kawauchi Y, Furukawa H, Sumiyoshi T, Gong JP, Osada Y. Necking phenomenon of double-network gels. Macromolecules 2006;39:4641–5.
[5] Na Y, Kurokawa T, Katsuyama Y, Tsukeshiba H, Gong JP, Osada Y, Okabe S, Karino T, Shibayama M. Structural characteristics of double network gels with extremely high mechanical strength. Macromolecules 2004;37:5370–4.
[6] Gong JP, Katsuyama Y, Kurokawa T, Osada Y. Double network hydrogels with extremely high mechanical strength. Adv Mater (Weinheim, Germany) 2003;15:1155–8.
[7] Nakajima T, Kurokawa T, Ahmed S, Wu W, Gong JP. Characterization of internal

fracture process of double network hydrogels under uniaxial elongation. Soft Matter 2013;9:1955–66.
[8] Hu J, Kurokawa T, Nakajima T, Sun TL, Suekama T, Wu ZL, Liang SM, Gong JP. High fracture efficiency and stress concentration phenomenon for microgel-reinforced hydrogels based on double-network principle. Macromolecules 2012;45:9445–51.
[9] Slaughter BV, Khurshid SS, Fisher OZ, Khademhosseini A, Peppas NA. Hydrogels in regenerative medicine. Adv Mater 2009;21:3307–29.
[10] Hoffman AS. Hydrogels for biomedical applications. Adv Drug Deliv Rev 2002;54(1):3–12.
[11] Kapoor S, Kundu SC. Silk protein-based hydrogels: promising advanced materials for biomedical applications. Acta Biomater 2016;31:17–32.
[12] Annabi N, Tamayol A, Uquillas JA, Akbari M, Bertassoni LE, Cha C, Camci-Unal G, Dokmeci MR, Peppas NA, Khademhosseini A. 25th anniversary article: rational design and applications of hydrogels in regenerative medicine. Adv Mater 2014;26(1):85–124.
[13] Tanaka Y. A local damage model for anomalous high toughness of double-network gels. Lett J Explor Front Phys (Europhys Lett) 78.
[14] Brown HR. A model of the fracture of double network gels. Macromolecules 2007;40:3815–8.
[15] Wang X, Hong W. Pseudo-elasticity of a double network gel. Soft Matter 2011;7:8576.
[16] Zhao X. A theory for large deformation and damage of interpenetrating polymer networks. J Mech Phys Solids 2012;60:319–32.
[17] Arruda EM, Boyce MC. A three-dimensional constitutive model for the large stretch behavior of rubber elastic materials. J Mech Phys Solids 1993;41:389. https://doi.org/10.1016/0022-5096(93)90013-6.
[18] Marckmann G, Verron E, Gornet L, Chagnon G, Charrier P, Fort P. A theory of network alteration for the Mullins effect. J Mech Phys Solids 2002;50:2011. https://doi.org/10.1016/S0022-5096(01)00136-3.
[19] Chagnon G, Verron E, Marckmann L, Gornet G. Development of new constitutive equations for the Mullins effect in rubber using the network alteration theory. Int J Solids Struct 2006;43:6817. https://doi.org/10.1016/j.ijsolstr.2006.02.011.
[20] Mao Y, Lin S, Zhao X, Anand L. A large deformation viscoelastic model for double-network hydrogels. J Mech Phys Solids 2017;100:103–30.
[21] Lu T, Wang J, Yang R, Wang T. A constitutive model for soft materials incorporating viscoelasticity and Mullins effect. J Appl Mech 2017;84(2):021010 .
[22] Wool RP. Self-healing materials: a review. Soft Matter 2008;4(3):400–18.
[23] Bergman SD, Wudl F. Mendable polymers. J Mater Chem 2008;18(1):41–62.
[24] Webber RE, Creton C, Brown HR, Gong JP. Large strain hysteresis and Mullins effect of tough double-network hydrogels. Macromolecules 2007;40:2919–27.
[25] Sun J-Y, Zhao X, Illeperuma WR, Chaudhuri O, Oh KH, Mooney DJ, Vlassak JJ, Suo Z. Highly stretchable and tough hydrogels. Nature 2012;489(7414):133–6.
[26] Yasuda K, Kitamura N, Gong JP, Arakaki K, Kwon HJ, Onodera S, Chen YM, Kurokawa T, Kanaya F, Ohmiya Y, Osada Y. A novel double-network hydrogel induces spontaneous articular cartilage regeneration in vivo in a large osteochondral defect. Macromol Biosci 2009;9:307–16.
[27] Keplinger C, Sun J-Y, Foo CC, Rothemund P, Whitesides GM, Suo Z. Stretchable, transparent, ionic conductors. Science 2013;341(6149):984–7.
[28] Darnell MC, Sun J-Y, Mehta M, Johnson C, Arany PR, Suo Z, Mooney DJ. Performance and biocompatibility of extremely tough alginate/polyacrylamide hydrogels. Biomaterials 2013;34(33):8042–8.
[29] Huebsch N, Kearney CJ, Zhao X, Kim J, Cezar CA, Suo Z, Mooney DJ. Ultrasound-triggered disruption and self-healing of reversibly cross-linked hydrogels for drug delivery and enhanced chemotherapy. Proc Natl Acad Sci 2014;111(27):9762–7.
[30] Hui C-Y, Long R. A constitutive model for the large deformation of a self-healing gel. Soft Matter 2012;8(31):8209–16.
[31] Long R, Mayumi K, Creton C, Narita T, Hui C-Y. Time dependent behavior of a dual cross-link self-healing gel: theory and experiments. Macromolecules 2014;47(20):7243–50.
[32] Guo J, Long R, Mayumi K, Hui C-Y. Mechanics of a dual cross-link gel with dynamic bonds: steady state kinetics and large deformation effects. Macromolecules 2016;49(9):3497–507.
[33] Wang Q, Gao Z. A constitutive model of nanocomposite hydrogels with nanoparticle crosslinkers. J Mech Phys Solids 2016;94:127–47.
[34] Nakajima T, Fukuda Y, Kurokawa T, Sakai T, Chung U, Gong JP. Synthesis and fracture process analysis of double network hydrogels with a well-defined first network. ACS Macro Lett 2013;2:518–21.
[35] Mullins L. Softening of rubber by deformation. Rubber Chem Technol 1969;42(1):339–62.
[36] Mullins L, Tobin N. Stress softening in rubber vulcanizates. Part i. Use of a strain amplification factor to describe the elastic behavior of filler-reinforced vulcanized rubber. J Appl Polym Sci 1965;9(9):2993–3009.
[37] Mullins L, Tobin N. Theoretical model for the elastic behavior of filler-reinforced vulcanized rubbers. Rubber Chem Technol 1957;30:551.
[38] Mullins L, Tobin N. Theoretical model for the elastic behavior of fillerreinforced vulcanized rubbers. Proceedings of the Third Rubber Technological Conference. 1954. p. 397.
[39] Diani J, Fayolle B, Gilormini P. A review on the Mullins effect. Eur Polym J 2009;45(3):601–12.
[40] Qi H, Boyce M. Constitutive model for stretch-induced softening of the stress-stretch behavior of elastomeric materials. J Mech Phys Solids 2004;52(10):2187–205.
[41] Ogden R, Roxburgh D. A pseudo-elastic model for the Mullins effect in filled rubber. Proc R Soc Edinburgh Sect: A 1999;455:2861. https://doi.org/10.1098/rspa.1999.0431.
[42] Zúñiga A, Beatty M. A new phenomenological model for stress-softening in elastomers. Z Angew Math Phys 2002;53(5):794–814.
[43] Elías-Zúñiga A. A phenomenological energy-based model to characterize stress-softening effect in elastomers. Polymer 2005;46(10):3496–506.
[44] Cantournet S, Desmorat R, Besson J. Mullins effect and cyclic stress softening of filled elastomers by internal sliding and friction thermodynamics model. Int J Solids Struct 2009;46(11):2255–64.
[45] Bueche F. Molecular basis for the Mullins effect. J Appl Polym Sci 1960;10:107–14.
[46] Govindjee S, Simo J. A micro-mechanically based continuum damage model for ccarbon black-filled rubbers incorporating Mullins' effect. J Mech Phys Solids 1991;39:87–112.
[47] Govindjee S, Simo J. Transition from micro-mechanics to computationally efficient phenomenology: carbon black filled rubbers incorporating Mullins' effect. J Mech Phys Solids 1992;40(1):213–33.
[48] Miehe C, Göktepe S, Lulei F. A micro-macro approach to rubber-like materials-part i: the non-affine micro-sphere model of rubber elasticity. J Mech Phys Solids 2004;52(11):2617–60.
[49] Miehe C, Göktepe S. A micro-macro approach to rubber-like materials. Part ii: the micro-sphere model of finite rubber viscoelasticity. J Mech Phys Solids 2005;53(10):2231–58.
[50] Göktepe S, Miehe C. A micro-macro approach to rubber-like materials. Part iii: the micro-sphere model of anisotropic Mullins-type damage. J Mech Phys Solids 2005;53:2259–83.
[51] Dargazany R, Itskov M. A network evolution model for the anisotropic Mullins effect in carbon black filled rubbers. Int J Solids Struct 2009;46:2967–77.
[52] Dargazany R. Multi-scale constitutive modeling of carbon-black filled elastomers (Ph.D. thesis). RWTH Aachen University; 2011.
[53] Göktepe S. Micro-macro approaches to rubbery and glassy polymers: predictive micromechanically-based models and simulations (Ph.D. thesis). University of Stuttgart; 2007.
[54] Bueche F. Mullins effect and rubber-filler interaction. J Appl Polym Sci 1961;15:271–81.
[55] Külcü ID. A micro-mechanically based modeling of double network hydrogels (Ph.D. thesis). RWTH Aachen University; 2016.
[56] Puso M. Mechanistic constitutive models for rubber elasticity and viscoelasticity (Ph.D. thesis). Lawrence Livermore National Laboratory, University of California Davis; 2003.
[57] Dargazany R, Khiêm VN, Navrath U, Itskov M. Network evolution model of anisotropic stress softening in filled rubber-like materials; parameter identification and finite element implementation. J Mech Mater Struct 2013;7(8):861.
[58] Bažant P, Oh B. Efficient numerical integration on the surface of a sphere. Z Angew Math Mech 1986;66:37.
[59] Ninan K, Nair C. Thermal decomposition studies. Part xii. Kinetics of dehydration of calcium oxalate monohydrate. multiple correlation with heating rate and sample mass. Thermochim Acta 1980;37(2):161–72.
[60] Sun J-Y, Zhao X, Illeperuma WR, Oh KH, Vlassak JJ, Suo Z. Interpenetrating networks with covalent and ionic crosslinks. uS Patent App. 14/370451; 2013.